Nanoparticle Size Is a Critical Physicochemical Determinant of the Human Blood Plasma Corona: A Comprehensive Quantitative Proteomic Analysis

Stefan Tenzer,[†,‡] Dominic Docter,[§,‡] Susanne Rosfa,[†] Alexandra Wlodarski,[†] Jörg Kuharev,[†] Alexander Rekik,[§] Shirley K. Knauer,[⊥] Christoph Bantz,[∥] Thomas Nawroth,[#] Carolin Bier,[§] Jarinratn Sirirattanapan,[△,▽] Wolf Mann,[△] Lennart Treuel,[□] Reinhard Zellner,[□] Michael Maskos,[∥,○] Hansjörg Schild,[†] and Roland H. Stauber[§,*]

[†]Institute for Immunology, University Medical Center of the Johannes-Gutenberg University Mainz, Langenbeckstrasse 1, 55101 Mainz, Germany, [§]Molecular and Cellular Oncology/Mainz Screening Center (MSC), University Medical Center of the Johannes-Gutenberg University Mainz, Langenbeckstrasse 1, 55101 Mainz, Germany, [⊥]Institute for Molecular Biology, Centre for Medical Biotechnology (ZMB), University Duisburg—Essen, Universitätsstrasse, 45117 Essen, Germany, [∥]Institute of Physical Chemistry, University Mainz, Jakob Welder Weg 11, 55099 Mainz, Germany, [#]Department of Biopharmaceutics and Pharmaceutical Technology, Institute for Pharmacy, University Mainz, Staudingerweg 5, 55099 Mainz, Germany, [△]Department of Otorhinolaryngology, Head and Neck Surgery, University Hospital of Mainz, Langenbeckstrasse 1, 55101 Mainz, Germany, [▽]Faculty of Medicine, Srinakharinwirot University, Sukhumwit 23, Wattana, Bangkok 10110, Thailand, [□]Institute for Physical Chemistry and Center for Nanointegration Duisburg—Essen (CeNIDE), University of Duisburg—Essen, Universitaetsstrasse 5-7, 45117 Essen, Germany, and [○]BAM, Bundesanstalt für Materialforschung und -prüfung, Division 6.3 Durability of Polymers, Unter den Eichen 87, 12205 Berlin, Germany. [‡]These authors contributed equally.

ABSTRACT In biological fluids, proteins associate with nanoparticles, leading to a protein "corona" defining the biological identity of the particle. However, a comprehensive knowledge of particle-guided protein fingerprints and their dependence on nanomaterial properties is incomplete. We studied the long-lived ("hard") blood plasma derived corona on monodispersed amorphous silica nanoparticles differing in size (20, 30, and 100 nm). Employing label-free liquid chromatography mass spectrometry, one- and two-dimensional gel electrophoresis, and immunoblotting the composition of the protein corona was analyzed not only qualitatively but also quantitatively. Detected proteins were bioinformatically classified according to their physicochemical and biological properties. Binding of the 125 identified proteins did not simply reflect their relative abundance in the plasma but revealed an enrichment of specific lipoproteins as well as proteins involved in coagulation and the complement pathway. In contrast, immunoglobulins and acute phase response proteins displayed a lower affinity for the particles. Protein decoration of the negatively charged particles did not correlate with protein size or charge, demonstrating that electrostatic effects alone are not the major driving force regulating the nanoparticle—protein interaction. Remarkably, even differences in particle size of only 10 nm significantly determined the nanoparticle corona, although no clear correlation with particle surface volume, protein size, or charge was evident. Particle size quantitatively influenced the particle's decoration with 37% of all identified proteins, including (patho)biologically relevant candidates. We demonstrate the complexity of the plasma corona and its still unresolved physicochemical regulation, which need to be considered in nanobioscience in the future.

KEYWORDS: bionanoscience · liquid chromatography mass spectrometry · nanotoxicity · nanomedicine · immunology · colloidal chemistry · bioinformatics

Besides the wide use of nanomaterials in industrial products, nano-enabled drug delivery systems are currently gaining applications also in the pharmaceutical industry.[1] Nanoparticle-based drugs are expected to display improved solubility, pharmacokinetics, and biodistribution and, thus, may be easier to administer with fewer side effects.[1,2] The ability to manipulate particular nanoparticle features such as their physical, chemical, and biological properties opens up a plethora of possibilities in rationally designing nanoparticles for drug delivery, as imaging agents, or for diagnostic purposes.[3−6]

When nanoparticles enter a biological fluid, proteins and other biomolecules rapidly compete for binding to the nanoparticle surface, leading to the formation of a dynamic protein corona that critically defines the biological identity of the particle. The biophysical properties of such a particle—protein complex often differ significantly from those of the formulated particle. Hence, the further biological responses of the body as well as the particle's biodistribution are significantly influenced by the nanoparticle—protein complex, potentially contributing also to unwanted biological side-effects.[7,8]

Particle material, size, and surface properties have been suggested to play a role in determining the composition of the corona, although the underlying physical mechanism is not yet fully resolved.[9−11] The term "hard corona" defines the long-lived equilibrium state, representing a protein signature of a nanoparticle in a certain environment.[12] Dissecting the composition of the protein corona in a given biological fluid may allow predictions of the particle's

* Address correspondence to rstauber@uni-mainz.de.

Received for review May 27, 2011 and accepted August 3, 2011.

Published online August 25, 2011
10.1021/nn201950e

fate regarding its interactions with specific cell types and surface receptors as well as predictions of its half-life in the body.[13,14]

For medical applications, nanoparticles are frequently administered parenterally. As the complete plasma proteome reference set contains almost two thousand proteins,[15] the plasma protein corona is expected to be complex as well.[16−20] Human plasma proteins play important roles in recognizing foreign materials entering the circulation.[21] Specific proteins are involved in eliciting an immunological response to pathogens or in assisting their clearance by the reticuloendothelial system.[13,21] Also, the nanoparticle's decoration with certain plasma proteins and/or blood components may influence uptake as well as clearance and, hence, potentially affect distribution and delivery to the intended target sites.[22,23] Thus, a deep understanding of the biological effects triggered by nanoparticles requires detailed knowledge of the particle-associated proteins, a fundamental prerequisite for nanobiology, nanomedicine, and nanotoxicology.[8,21,24]

To date, various studies have been conducted to identify plasma proteins associating with nanoparticles and attempted to correlate their binding with the physicochemical properties of the particles.[11,12,18,25] Mostly, protein adsorption on nanostructured surfaces has not been quantitatively characterized, resulting in an incoherent picture of how the particle's physicochemical properties mechanistically affect the composition of the protein corona.

To fill this gap, we here employed comprehensive experimental approaches to not only qualitatively but also quantitatively dissect the composition of the human plasma protein corona formed on commercially widely used amorphous silica nanoparticles (SiNPs) and its dependence on nanoparticle size. Proteins in the corona that are conserved or unique across the nanoparticle types were identified and bioinformatically classified according to their functional properties, and the obtained results were compared to the current literature. To our knowledge, this is the first comprehensive study reporting an absolute quantification of the size-dependent blood-plasma-derived protein corona by quantitative label-free liquid chromatography mass spectrometry.

RESULTS

Silica Nanoparticles. In contrast to other studies addressing particles varying in numerous physicochemical properties, such as material, size, surface modification, or charge,[9,12,18] we here focused exclusively on amorphous silica nanoparticles that differ only in size. We feel that reducing nanoparticle variability to a single parameter is required to reliably identify nanoparticle properties affecting the protein corona composition.

As a thorough characterization of nanomaterials is an absolute prerequisite for all studies, we first determined critical properties of the particles by independent experimental methods. According to transmission electron microscopy (TEM), dynamic light scattering (DLS), and zeta potential measurements, the respective particles were homogeneous and monodisperse, and all displayed a negative surface charge (Table 1 and Figure 1A). Electron microscopy conclusively confirmed the spherical shape of the SiNPs (Figure 1A). No evidence of agglomerates was observed when dispersed in water or in physiological buffer (buffer A), confirming the stability of the particle suspensions. In contrast to other investigations reporting significant deviations from nominal specifications with commercially supplied samples,[9,12] the material selected for this study fulfilled critical quality criteria and thus served as a model system.

TABLE 1. SiNP Characterization

	TEM[a]	DLS[a]	Zetasizer
	radius ± SD [nm]	hydrodynamic radius $\langle R_h \rangle_z$ [nm]	μ_2 zeta potential ζ [mV]
SiNP	in dry state	in buffer A	in buffer A
SiNP-8	9.6 ± 2.2	12.5 ± 0.19	-11 ± 5
SiNP-20	15.7 ± 1.9	17.6 ± 0.1	-25 ± 6
SiNP-125	54.9 ± 17.2	71.3 ± 0.05	-32 ± 4

[a] The average size of the three different SiNPs was determined in dry state (TEM) as well as in buffer A by DLS. Values are mean ± SD from three independent experiments.

SiNPs Efficiently Bind Plasma Proteins. Subsequently, particles were incubated with human plasma for one hour followed by centrifugation to pellet the particles and extensive washing to remove all unbound proteins. Prior to performing a comprehensive analysis of the plasma protein corona for the respective SiNPs, we first applied one- and two-dimensional polyacrylamide gel electrophoresis (2D-PAGE), to demonstrate stable and particle size-dependent protein signatures (Figure 1B and C). Kinetic studies further showed that the plasma corona formed rapidly and was stable over time (Supplementary Figure S1A, and data not shown).

Dissecting the Hard Blood Plasma-Derived Corona by Quantitative Mass Spectrometry. To allow not only a qualitative but also a sensitive and quantitative analysis of the plasma protein corona, we next used label-free liquid chromatography mass spectrometry (LC-MS). Although other studies identified numerous proteins in the hard corona,[13,26,27] we here reliably detected and quantified 125 different proteins. Each sample was analyzed in at least three technical replicates. The obtained results were confirmed by independent measurements, and the high correlation coefficient ($R^2 > 0.98$) between technical replicates underlines the quality and reproducibility of our analysis (Supplementary Figure S2). The full list of identified proteins including their calculated isoelectric point (pI)

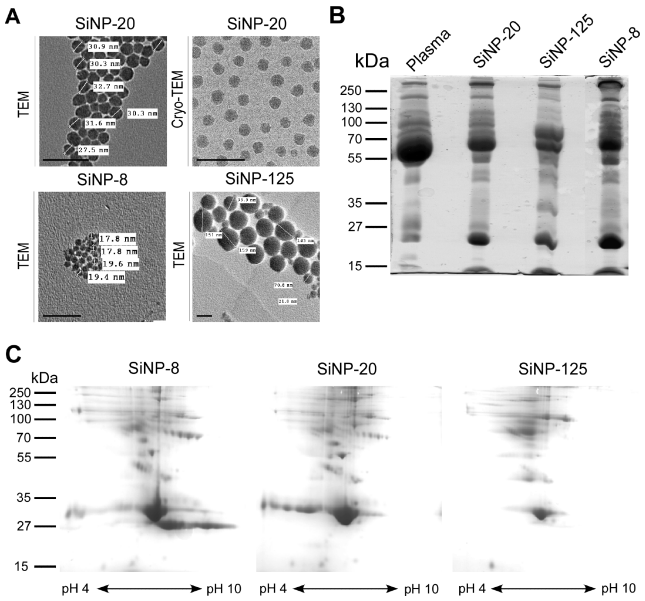

Figure 1. Characterization and plasma protein binding profiles of SiNPs. (A) Analysis of SiNPs varying in size by TEM and Cryo-TEM. Bars = 100 nm. (B/C) Gel electrophoresis to visualize SiNP-bound human plasma proteins. Proteins were separated by 1D- (B) or 2D-SDS-PAGE (C) and visualized by Coomassie (B) or SYPRO-orange (C) staining. MW is indicated.

TABLE 2. List of the 20 Most Abundant Proteins (decreasing from 1 to 20) Detected in the SiNP-125 Corona or in Crude Plasma by LC-MS[a]

MW	pI	SiNP-125	no.	plasma	pI	MW
69 365	**5.85**	**serum albumin**	1	**serum albumin**	**5.85**	**69 365**
30 777	**5.35**	**apolipoprotein A-I**	2	**alpha-2-macroglobulin**	**5.97**	**163 276**
70 036	5.48	prothrombin	3	**complement C3**	**5.96**	**187 145**
515 556	6.62	apolipoprotein B-100	4	**Ig gamma-1 chain C region**	**8**	**36 105**
187 145	**5.96**	**complement C3**	5	serotransferrin	6.73	77 049
139 094	**6.18**	**complement factor H**	6	alpha-1-antitrypsin	5.17	46 735
1 011 016	5.14	nesprin-1	7	haptoglobin	6.14	45 204
129 381	4.49	thrombospondin-1	8	**apolipoprotein A-I**	**5.35**	**30 777**
262 603	5.26	fibronectin	9	Ig kappa chain C region	5.47	11 608
85 696	5.83	gelsolin	10	Ig gamma-2 chain C region	7.3	35 900
55 153	6.1	plasma protease C1 inhibitor	11	complement C4-A	6.65	192 769
103 356	6.54	interalpha-trypsin inhibitor heavy chain H4	12	Ig alpha-1 chain C region	6.06	37 654
163 276	**5.97**	**alpha-2-macroglobulin**	13	Ig gamma-4 chain C region	7.03	35 940
453 662	4.61	A-kinase anchor protein 9	14	hemopexin	6.58	51 675
77 153	9.28	twinkle protein, mitochondrial	15	ceruloplasmin	5.29	122 203
71 956	6.37	kininogen-1	16	Ig lambda chain C regions	6.96	11 236
144 737	7.71	shugoshin-like 2	17	alpha-1-antichymotrypsin	5.11	47 650
36 105	**8**	**Ig gamma-1 chain C region**	18	interalpha-trypsin inhibitor heavy chain H2	6.42	106 462
36 153	5.36	apolipoprotein E	19	**complement factor H**	**6.18**	**139 094**
52 601	6.29	antithrombin-III	20	Ig mu chain C region	6.34	49 306

[a] Bold proteins were found in both groups. pI: isoelectric point. MW: molecular weight. For further details see Supplementary Table S1.

and molecular weight (MW) as well as their relative abundance can be found in Supplementary Table S1. First, this analysis showed that the obtained binding profiles did not simply correspond to the relative protein concentrations in the plasma preparations, as observed before by other studies investigating other types of nanomaterials (Table 2 and Supplementary Table S1).[11,12,18,25] Although serum albumin as the protein with highest concentration in the plasma was also the most abundant protein detected in the corona of all SiNPs, the second most abundant plasma protein, α-2-macroglobulin, was only the 13th most abundant protein detectable on SiNP-125. Previous reports suggested that negatively charged particles attract primarily positively charged proteins.[13,21,26,28] Such a particle decoration might subsequently facilitate the interaction with the negatively charged cell surface, thereby facilitating particle uptake.[13,21,26] In contrast, our results now exclude an enhanced binding of positively charged plasma proteins at pH 7.3, *i.e.*, the

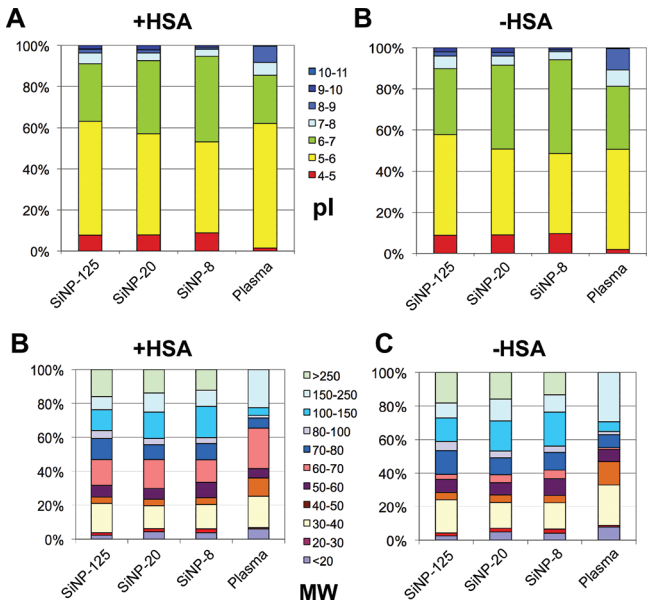

Figure 2. Comparison and characterization of SiNP-specific protein signatures identified by quantitative mass spectrometry. Proteins were classified according to their calculated isoelectric point (pI) (A/B) or molecular weight (MW) (C/D), and their relative percentages are shown. (A/B) At pH 7.3 (pH measured in plasma) SiNPs preferentially bound negatively charged proteins (pI < 7). Compared to plasma, proteins with pI < 5 were enriched in the protein corona, independent of particle size. (C/D) No significant, distinct protein size-dependent particle binding pattern was observed. Proteins with high molecular weight being almost undetectable in plasma were significantly enriched, while proteins with low molecular weight were less abundant compared to plasma. Similar signatures were observed when the protein binding profiles were *in silico* corrected for human serum albumin (B/D: −HSA).

pH present in plasma preparations (Figure 2A). Instead, we noticed that, overall, proteins displaying a negative charge (pI < 7) were preferentially bound by the negatively charged SiNPs used in this study, irrespective of their relative abundance in the plasma (Table 2 and Supplementary Table S1). Similar results were found when the protein binding profiles were *in silico* corrected for the highly abundant protein serum albumin (Figure 2B). This result was independently confirmed by zeta potential measurements, revealing a negative charge of protein-covered SiNPs (SiNP-20: $\zeta = -12.2$ mV; data not shown). Also, we noticed that proteins with pI < 5 were concentrated in the protein corona independent of particle size, while proteins with pI > 7 were less enriched (Figure 2A/B, and Supplementary Table S1). Hence, effective charge alone appears not to be the major driving force regulating the SiNP−protein interaction. Third, our data did not indicate a distinct, protein size-dependent particle binding effect, although we observed a significant enrichment of plasma proteins with high MW (Figure 2C/D). Fourth, proteins being close to or below detection limits in crude plasma preparations were significantly enriched and reliably detectable upon incubation with SiNPs (Supplementary Table S1). For example, plasma exposure to SiNP-125 resulted in a 35-fold enrichment of prothrombin (Supplementary Table S1). As such, enrichment by SiNPs allowed the detection of 125 different proteins, whereas we could detect only 86 different proteins in crude plasma due to the high dynamic range of the plasma proteome (Figure 2C). Similar enrichment effects have been observed for other nanomaterials in other studies.[11,12,18,25,28]

Classification of Bound Plasma Proteins. Next, we employed bioinformatic tools, such as the GeneSpring GX and the Ingenuity "Pathway and Network Analysis" software, to classify the bound proteins according to their proposed GO terms, such as subcellular localization and molecular and biological functions. As shown in Supplementary Table S1, the majority of the detected proteins were bioinformatically correctly classified as proteins localizing to the extracellular region or space, underlining the reliability of our analysis. On the basis of their proposed molecular function, most proteins were predicted to act via protein binding, by the regulation of protease activity, or by influencing calcium and lipid signaling (Supplementary Table S1).

Also, this unbiased analysis confirmed that the functions of the identified corona components are associated with biological processes of the blood system such as complement activation, immune responses, lipid and cholesterol metabolism, coagulation, and acute phase response (Supplementary Table S1). Notably, this analysis revealed a significant enrichment of plasma proteins involved in complement activation (Figure 3B), lipoproteins (Figure 3C), or coagulation (Figure 3D). The also significantly enriched group of "tissue leakage" proteins contains several proteins with potential disease-relevant functions (Figure 3G). In contrast, although immunoglobulins (Figure 3E), acute phase

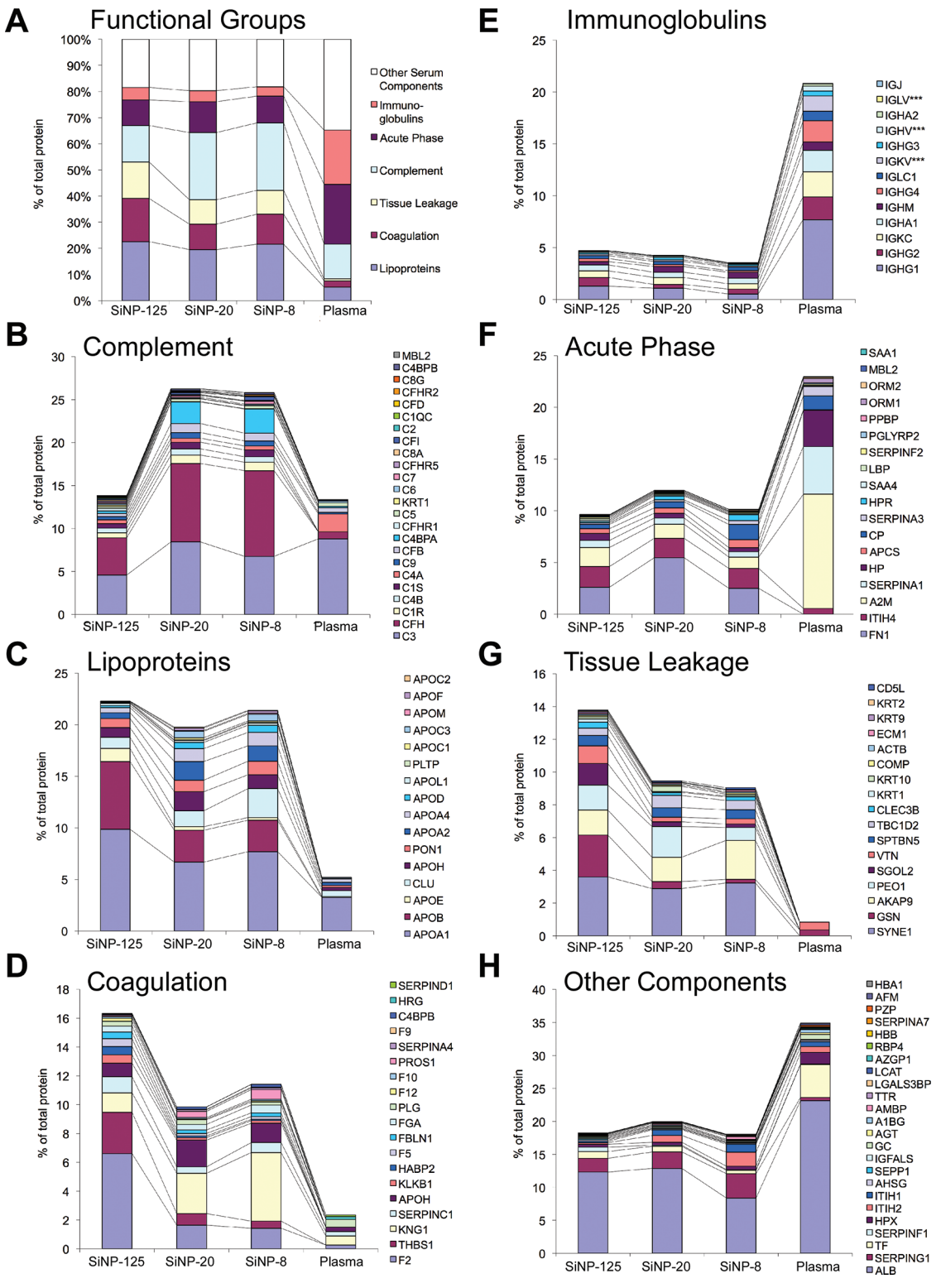

Figure 3. Bioinformatic classification of identified corona proteins according to their functions. Employing bioinformatic tools, proteins identified in the respective SiNPs corona were classified according to biological processes of the blood system (A). The relative percentages of the proteins compared to crude plasma are shown. A significant enrichment of plasma proteins involved in complement activation (B), lipoproteins (C), coagulation (D) as well as proteins grouped as "tissue leakage" (G) was evident in the corona. Although immunoglobulins (E), acute phase response proteins (F), and serum albumin (H) were present in high amounts in the plasma, these proteins displayed a lower affinity for the SiNPs.

response proteins (Figure 3F), and serum albumin (Figure 3H, ALB) were present in high amounts in the plasma, these proteins displayed a lower affinity for the SiNPs investigated.

TABLE 3. Selection of Identified Proteins on the SiNPs, Grouped According to Their Function[a]

Function	pI	MW	SiNP-8	SiNP-20	SiNP-125
Immunoglobulins					
Ig gamma-1 chain C region	8.00	36105	+	++	++
Ig gamma-2 chain C region	7.30	35900	+	+	++
Lipoproteins					
Apolipoprotein A-II	6.42	11174	++	++	+
Apolipoprotein A-IV	5.00	45398	++	++	+
Apolipoprotein B-100	6.62	515556	+	+	++
Apolipoprotein C-I	8.85	9331	++	+++	+
Apolipoprotein C-III	5.00	10852	+++	+++	+
Apolipoprotein D	4.77	21275	++	++	+
Apolipoprotein E	5.36	36153	+	+	++
Apolipoprotein F	5.06	33462	+++	+++	+
Beta-2-glycoprotein 1	7.71	38297	+	++	+
Clusterin	5.83	52494	++	+	+
Coagulation					
Antithrombin-III	6.29	52601	+	+	++
Coagulation factor V	5.60	251668	+	+	++
Coagulation factor XII	7.42	67817	+	+	++
Hyaluronan-binding protein 2	6.10	62671	+	+	+++
Kininogen-1	6.37	71956	++	+	+
Plasma kallikrein	7.94	71368	+	+	++
Prothrombin	5.48	70036	+	+	+++
Thrombospondin-1	4.49	129381	+	++	+++
Vitamin K-dependent protein S	5.26	75121	+++	++	+
Complement					
C4b-binding protein alpha chain	6.93	67032	+++	+++	+
C4b-binding protein beta chain	4.75	28357	+++	+++	+
Complement C1r subcomponent	5.77	80117	++	++	+
Complement C3	5.96	187145	+	++	+
Complement factor B	6.65	85531	++	++	+
Complement factor H	6.18	139094	++	++	+
Complement factor H-related protein 1	7.08	37650	+	+	+++
Complement factor I	7.18	65719	++	++	+
Keratin, type II cytoskeletal 1	8.10	66037	+	+	++
Acute Phase					
Alpha-1-antichymotrypsin	5.11	47650	++	+	+
Ceruloplasmin	5.29	122203	++	+	+
Fibronectin	5.26	262603	+	++	+
Haptoglobin-related protein	6.46	39007	++	++	+
Serum amyloid A-4 protein	9.70	14806	+	+	++
Cellular Component					
Gelsolin	5.83	85696	+	+	+++
Keratin, type I cytoskeletal 10	4.78	58852	+	++	+
Shugoshin-like 2	7.71	144737	+	+	+++
Twinkle protein, mitochondrial	9.28	77153	+	++	++
Vitronectin	5.38	54304	+	+	++
Other Serum components					
Inter-alpha-trypsin inhibitor heavy chain H1	6.34	101387	+++	++	+
Inter-alpha-trypsin inhibitor heavy chain H2	6.42	106462	+++	++	+
Pigment epithelium-derived factor	5.94	46341	+	++	+++
Protein AMBP	5.83	38999	++	+	+
Selenoprotein P	7.58	43173	+	+	++
Serotransferrin	6.73	77049	+	+	++

[a] +: defined as 1. ++: fold change ≥2−5×. +++: fold change >5×. The binding of 46 proteins is significantly affected by the particle size. pI: isoelectric point. MW: molecular weight.

Particle Size Critically Determines the Binding of Plasma Proteins. Importantly, our analysis revealed that the binding of 37% of all corona proteins identified is significantly affected by particle size (Table 3). These proteins do not cluster to a distinct functional class but are distributed across all biological processes (Table 3). A general comparison of the degree of similarity of the protein corona around the different SiNPs is presented

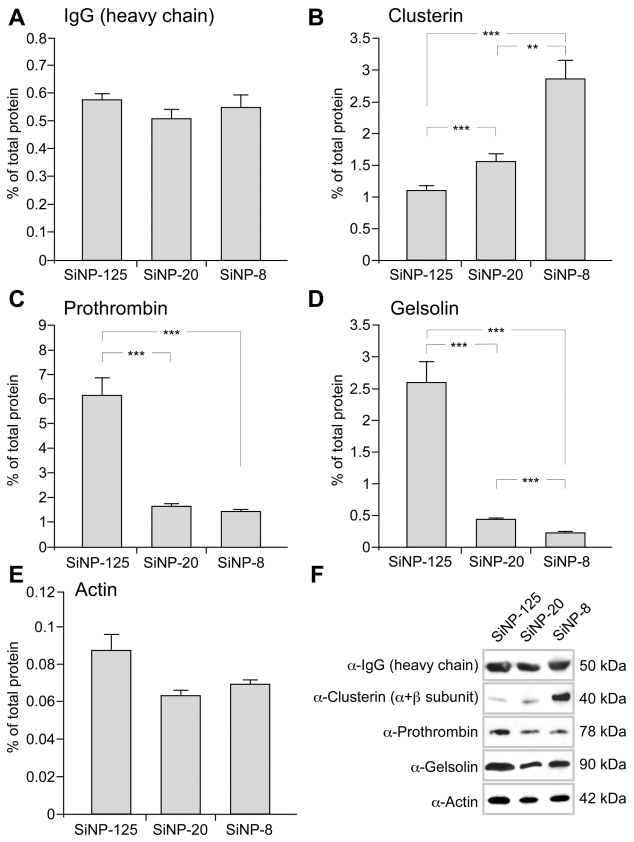

Figure 4. Particle size-dependent composition of the blood-plasma corona. Binding affinities of selected proteins verified by independent experimental methods (A−E, LC-MS; F, immunoblot analysis). IgG and actin served as controls. Columns, mean; bars, ±SD from six independent experiments (A−E). (A/E) IgG and actin showed no significant particle size-depending binding. (B) The lipoprotein clusterin showed a highly significant enhanced affinity for the small SiNP-8 ($p < 0.01$; ***$p < 0.001$). (C/D) Prothrombin and gelsolin preferentially bound to the large SINP-125 (***$p < 0.001$). (F) Semiquantitative immunoblot analyses confirmed the results obtained by LC-MS. MW is indicated.**

in Figure 3. Remarkably, even differences in particle size of only 10 nm significantly affected the nanoparticle corona as exemplified by the differential binding of gelsolin, clusterin, or prothrombin (Figures 3 and 4). We identified not only proteins showing enhanced binding to the larger SiNP-125 but also candidates with higher affinities for the smaller particles (Table 3, Figures 3 and 4).

Due to the higher surface curvature of small nanoparticles, it could be assumed that smaller proteins are also enriched on SiNP-8 and -20 compared to SiNP-125.[14,28] However, we did not notice such a protein size-dependent trend nor did the effective protein charge explain the observed particle size-dependent binding patterns (Supplementary Figure S3).

To further underline the reliability and thus relevance of our proteomic analysis, we verified the size-selective binding affinities by an independent experimental method. As shown in Figure 4F, immunoblot analysis confirmed the enhanced binding of the lipoprotein clusterin to the small SiNP-8, whereas prothrombin or the actin regulatory protein gelsolin preferentially bound to the larger SiNP-125. As a control, the binding of IgG or actin was not significantly affected by particle size, which is in line with the results obtained by mass spectrometry (Supplementary Table S1). Of note, absolute quantification by LC-MS allows one to reliably detect even small size-dependent differences in particle-binding affinities, which cannot be resolved by semiquantitative immunological methods.

DISCUSSION

Accurate and extensive mapping of the biomolecule corona around nanomaterials is becoming a key objective in the ample field of bionanoscience. Although several studies have been conducted to identify proteins associating with nanoparticles and to correlate their binding with the physicochemical properties of the particles, our understanding of these processes is far from being complete.[21] Hence, it is of utmost importance to comprehensively analyze not only the qualitative but also the quantitative composition of the protein corona. Consequently, we here used label-free liquid chromatography−mass spectrometry to determine the composition of the hard human plasma protein corona formed on commercially widely used amorphous silica nanoparticles as well as its dependence on nanoparticle size. To mimic the conditions in the

bloodstream, nanoparticles were incubated with plasma so that the plasma protein levels were in excess of the available particle surface area. Currently, several techniques are available for isolating nanoparticle−protein complexes, including equilibrium dialysis, size-exclusion chromatography, and microfiltration.[9,13,29] Each individual method has its advantages but also specific limitations in terms of reproducibility, sensitivity, and resolution.[9,13,29] As separation by centrifugation can easily be used routinely, was found here to be highly reproducible, and required relatively little material, we selected this approach. However, we are aware that the protein fingerprints identified here might vary to a certain degree when using other separation techniques.[30]

For protein separation and identification, most studies used 2D-PAGE, followed by mass spectrometry of individual excised protein spots.[9,13,18,26,31] We found that label-free LC-MS is highly reproducible and sensitive and appears to be less affected by the various caveats of 2D-PAGE, spot excision, and protein identification by subsequent mass spectrometry. Notably, the obtained quantitative results could be confirmed by independent complementary methods underlining the feasibility and analytical quality of our approach.

The complete composition of the protein corona at any given time is determined by the proteome, as well as by its kinetic properties (equilibrium constants, on/off rates, binding affinity) for the particular nanoparticles.[21,32] Several investigations showed that particle material, size, and surface properties can play a significant role in determining the composition of the corona.[9,12,13,26,30] However, the observations are not always consistent, and no distinct mechanisms explaining protein-specific binding have emerged from these studies. Some investigators found that for copolymer particles varying in diameter, the amount of bound protein varied with size and surface curvature, but that the protein pattern was identical for all sizes.[18] In contrast, other studies using similar polymer, gold, or other metal nanoparticles reported not only significant quantitative but also qualitative size-dependent changes in the obtained protein fingerprints.[12,13,26,33] So far, the underlying mechanisms for such somehow unexpected observations, which certainly include hydrophobic/hydrophilic as well as electrostatic interactions, are not yet resolved.[21,34] As a larger surface-to-volume ratio implies that more proteins may bind to smaller nanoparticles (relative to their mass) than to particles of larger size, the particle-specific differences in total surface area ($A = 4\pi R^2$) were discussed as a potential explanation.[12,13,26] Whereas this was confirmed for the binding of individual proteins,[32,35] no clear correlations could be obtained for complex protein mixtures.[12,13,26,30]

We clearly could quantitatively show for the SiNPs investigated that particle size predominantly affected the relative amounts of 46 proteins in the corona rather than having a significant qualitative impact. Also, we did not observe that the larger total surface area of the small SiNPs correlated with increased binding for all 46 proteins. Although total surface area most likely contributes to the particle specific binding for some proteins, this effect does not exclusively determine the complete corona. Concluding that particle size predominantly affects the protein corona quantitatively rather than qualitatively seems plausible, as no mechanisms have been shown so far explaining why size alone should either allow or completely abolish binding of certain proteins. Although we did not examine the protein binding profiles of particles for which qualitative size-dependent protein binding profiles have been reported, one might speculate that the reported "all or nothing effects" were also quantitative rather than qualitative. As such, "absent proteins" might be merely below the detection limits of the employed methods. Recent studies using variable plasma protein concentrations also observed a quantitative rather than qualitative effect on the corona.[30] Such investigations suggest an additional level of complexity, as variable biomolecule concentrations in biological fluids appear to have an additional impact on the dynamics of the nanoparticle corona over time.[30]

Currently, it is not known whether the detected proteins bind to the SiNPs as mono- or multilayers. Although the surface of small nanoparticles is limited, the surface of SiNP-8 would allow the binding of roughly one hundred serum albumin molecules (approximated by an equilateral triangular prism of 8 nm).[32,35] Hence, the formal possibility exists that the 125 proteins identified might bind as a monolayer.

Besides size, other particle characteristics such as material and surface properties have been suggested to affect the composition of the corona.[9,12,13,26,28,30] However, studies addressing the influence of surface charge density also reported various outcomes. For one, an increase in plasma protein absorption with surface charge density without affecting the overall protein profile was reported.[36] In contrast, other investigations found that modulating the surface charge of polystyrene nanoparticles significantly influenced the composition of the corona.[9,12,13] Also, positively charged polystyrene nanoparticles were reported to preferentially adsorb proteins with pI < 5.5, while negatively charged particles predominantly bound proteins with pI > 5.5.[31] We found that the corona of the negatively charged SiNPs investigated here is preferentially composed of proteins with pI < 7, displaying a negative charge at pH 7.3, *i.e.*, the pH present in plasma preparations. This overall negative surface charge of the decorated particles remains unchanged even if the binding profiles were corrected *in silico* for the most abundant protein serum albumin (pI = 5.8). Collectively, electrostatic effects alone do not

constitute the major driving force regulating the SiNP–protein interactions. Whether the observed preferential binding of negatively charged proteins can be explained by a sequential model of protein attachment, in which abundant positively charged serum proteins initially bind the SiNPs, thus coating the negative charges, followed by binding of anionic proteins to the cationic protein coat remains to be investigated. Also, whether positively charged domains are present on the surface of proteins in solution and as such may mediate the interaction with the negatively charged particle surface is not known.

In addition, the hydrophobicity of a nanoparticle surface has been shown to influence not only the amounts but also the identities of the bound proteins.[12,13] Less hydrophobic copolymer particles bound virtually no proteins, while more hydrophobic particles preferentially bound apolipoproteins and serum albumin.[18] Notably, all these proteins were also found to interact with the hydrophilic SiNPs in appreciable amounts.

Just as the nanoparticle properties dictate the extent and specificity of the protein binding profile, the protein corona rather than the bare particle will come into contact with biological systems and, thus, may determine biodistribution and trigger (patho)biological responses.[11,12,25,30] By identifying 125 proteins, we feel that we provide a quite comprehensive description of the blood plasma-derived corona. We are aware that the plasma corona may be even more complex, as some proteins may be below our detection limit. Although the complete plasma proteome is estimated to contain almost two thousand proteins competing for the limited space on a nanoparticle surface, one needs to bear in mind that many of them are present only in minute amounts.[15] Thus, suffice it to speculate that the candidates identified here will have physiological relevance.[37]

As such, binding of opsonins such as IgG and complement factors is expected to promote phagocytosis and the eventual removal of particles from systemic circulation via cells of the reticuloendothelial system, finally concentrating nanoparticles in the liver and spleen.[23,37] We not only found immunoglobulins associated with the corona of all three SiNPs but also observed particle size-dependent binding of several complement factors. Complement activation supports the cell-mediated and humoral immunity but is also responsible for allergic reactions and anaphylaxis.[27,37] Although the underlying molecular mechanisms are not yet resolved, complement activation by systemically administered nanomaterials has been reported.[27,37] On the other hand, albumin as the most abundant protein in plasma was associated with each SiNP at relatively high levels, in contrast to what was reported for metal oxide particles.[13,26] As dysopsonins such as albumin have been shown to promote prolonged nanoparticle circulation times in the blood,[13,26] these may antagonize the biological reactions triggered by SiNP-bound opsonins.

Notably, we observed particle size-dependent binding for several proteins involved in blood coagulation. Whereas significant enrichment of prothrombin and thrombospondin-1 was observed for SiNP-125, these proteins bound less to SiNP-20 and -8. Although *in vivo* data for the SiNPs are missing, one may speculate that an increase in the circulation time by bound dysopsonins commensurately increases the duration of contact with components of the coagulation system. Although some reports suggest that nanomaterials can indeed induce platelet aggregation, the underlying mechanisms are largely unknown.[26,27,38]

A functionally diverse group of plasma proteins that we found highly enriched in the corona of the SiNPs are apolipoproteins, involved in lipid and cholesterol transport and metabolism.[39,40] Several individual members of the apolipoprotein family as well as lipids have also been detected on other nanomaterials,[12,18,41] although we now identified 16 apolipoproteins in the SiNP corona. The size of the nanoparticles used in this study is of the same order as most of the various lipoprotein particles.[39,40] Lipoprotein particles selectively bind to receptors, and hence, the lipoproteins in the nanoparticle corona are expected to affect their biodistribution.[13,42] Also, the nature of the adsorbed proteins is suggestive of pathobiological conditions, such as cardiovascular and neurodegenerative disease risks, although any potential causal correlation demands further investigation.[40,43,44]

Among the proteins for which we and others observed significant particle size-dependent binding is plasma gelsolin, which has been implicated in a number of processes such as inflammation or extracellular signal transduction pathways.[12,45] The correlation between blood gelsolin levels and critical clinical conditions underlines its pathopysiological relevance.[46,47] Whether the plasma gelsolin enriched on SiNP-125 is still biologically active and may contribute to particle-induced biological effects has not been investigated.

CONCLUSIONS

Here, we present a quantitative comprehensive analysis of the protein corona in a physiologically relevant environment and of physicochemical nanoparticle parameters influencing its composition. We demonstrate how label-free liquid chromatography mass spectrometry combined with *in silico* analysis not only allows dissecting the complexity of the blood plasma-derived corona *in situ* but also provides an analytical and conceptual framework for the building of a knowledge-based *in vivo* hypothesis.

In summary, we convincingly show that (i) the blood plasma corona is highly complex; (ii) protein binding did not simply correlate with their relative abundance in the plasma; (iii) neither protein size nor charge significantly determined the protein fingerprints,

indicating that electrostatic effects alone do not constitute the major driving force regulating the corona; (iv) bioinformatic classification revealed an enrichment of lipoproteins, proteins involved in coagulation and the complement pathway, whereas immunoglobulin and acute phase response proteins displayed lower affinities for the particles; and (v) particle size critically determines quantitatively but not qualitatively the binding of 37% of all identified proteins.

By identifying 125 proteins in the corona, which may theoretically be present as a monolayer, we provide another though quite comprehensive data set facilitating the rational identification of proteins ultimately responsible for triggering (patho)biological responses. In nanomedicine, studies assessing many different nanoparticle types indicated that hydrophobicity, size, and surface charge are the main parameters influencing nanoparticle biocompatibility and toxicity.[2] Facing now the complexity of the plasma corona necessitates future investigations to determine whether and to what extent the biological effects observed are mediated by the biomolecule corona and/or the biophysical properties of the formulated nanomaterials.[11,25,28,30]

Our quantitative results will also guide the design and have deep implications for the interpretation and extrapolation of experimental outcomes investigating the impact of physicochemical parameters on the nanobio-interface both from the biological and from the material side. By applying quantitative LC-MS, the final goal is to define adsorption isotherms of the different biomolecule components of the adsorbed layer and to relate the amounts bound from LC-MS to those detected by structural/biological studies. Whereas models based on the Langmuir adsorption and other isotherms are being tested and constantly improved, the theoretical understanding and prediction why certain proteins are adsorbed in a competitive manner is the major challenge for the future.

Although the kinetics of protein binding was not investigated in detail, recent results demonstrate that the hard biomolecule corona forms rapidly and remains stable.[11,30] For model systems involving single proteins, excellent and elegant studies already exist.[32,35,48−50] However, we feel that studying the kinetics of comprehensive protein binding profiles by label-free LC-MS will provide novel insights closer to the physiological situation.[51]

On the basis of the results obtained from the studies performed so far, one clearly needs to consider the forces governing colloidal chemistry as well as the adaptations that occur at biological interfaces. Employing complementary experimental methods from the different disciplines is required to understand this collective process, which determines what is ultimately "seen" by the cell in nanobioscience.

METHODS

Amorphous Silica Nanoparticles. The SiNP-8, SiNP-20, and SiNP-125 aqueous silica dispersions were purchased from Nyacol Nano Technologies, Inc. (Ashland, MA, USA) and used as received. SiNPs were characterized with respect to shape, size, and size distribution in the dry state as well as in solution. Transmission electron microscopy imaging was performed using a Philips EM420 on carbon-coated copper grids as outlined.[52] The size and zeta potential for the SiNPs were determined with a Malvern Zetasizer NanoZS as described.[35,52,53] SiNPs were diluted with buffer A (103.5 mM NaCl, 5.3 mM KCl, 5.6 mM Na_2HPO_4, 1.4 mM KH_2PO_4, 23.8 mM $NaHCO_3$, pH 7.4), and measurements were conducted at 25 °C using 0.6 mg/mL SiNPs concentrations.

Human Plasma. Blood was taken at the ENT department at the Medical University Mainz from 15 different seemingly healthy donors in k2EDTA-coated tubes (Greiner Bioone, Germany) to prevent blood clotting. The blood samples were labeled anonymously and could not be traced back to a specific donor. Studies were performed according to the requirements of the local ethics committee, and informed consent was obtained in accordance with the Declaration of Helsinki. The tubes were centrifuged for 5 min at 4000 rpm to pellet red and white blood cells. The plasma supernatant was pooled, aliquoted, and stored at −80 °C. This pooled plasma was used exclusively throughout the study. After thawing the plasma was centrifuged for 2 min at 12 000 rpm/4 °C to further remove protein precipitates.

SiNP Incubation with Human Plasma. All experiments were conducted at least twice to ensure reproducibility. The ratio of total particle-surface area to plasma concentration was kept the same for the three different particle sizes to ensure comparability between the results. Therefore, the total surface area ($A = 4\pi R^2$) per particle mass was calculated for the individual SiNPs and adjusted to obtain a constant plasma volume to particle surface ratio of 5.55 mL/m^2 as described.[12] Particle suspensions were incubated with an equal amount of human plasma for 1 h at 4 °C (total volume 500 μL). The samples were centrifuged to pellet the particle−protein complexes (10 min at 12 000 rpm/4 °C). The pellet was resuspended in buffer A, transferred to a new vial, and centrifuged again to pellet the particle−protein complexes (10 min at 12 000 rpm/4 °C); this procedure was repeated three times. After the third washing step, the supernatant did not contain any detectable amount of proteins. Proteins were eluted from the particles by adding SDS-sample buffer (62.5 mM Tris-HCl pH 6.8; 2% w/v SDS, 10% glycerol, 50 mM DTT, 0.01% w/v bromophenol blue) to the pellet and incubating at 95 °C for 5 min.

SDS/PAGE (1D and 2D). Discontinuous SDS-polyacrylamide gel electrophoresis (PAGE) was carried out according to standard procedures.[54] Proteins were visualized by staining with Coomassie brilliant blue R-250 as described.[54] All experiments were conducted at least twice to ensure reproducibility of the results. Isoelectric focusing (IEF) and 2D-PAGE were performed as described previously.[55] Immobilized pH-gradient strips (IPG strips, pH 3−10) and carrier ampholytes (IPG buffer) were from Amersham Biosciences (Uppsala, Sweden). SYPRO Orange 5000× stock solution was purchased from Bio-Rad Laboratories (Munich, Germany). For IEF, 500 μg of total protein was used on the IPG-strip. Strips were equilibrated for 15 min using equilibration buffer (50 mM Tris, 6 M Urea, 2% SDS, 30% glycerol, 0.003% BPB; pH 8.8) including 1% DTT, followed by 15 min incubation in equilibration buffer including 2.5% iodoacetamide. The second dimension was applied on a 14.5% SDS gel. Gels were stained using staining solution (2% HOAc, 0.001% SDS, 1/4000 vol.

SYPRO orange). Scanning was performed on a flourescence scanner (Storm 840, Amersham Pharmacia, Freiburg).

Protein Digest Preparation. Proteins eluted from SiNPs (30 μg) or crude plasma proteins (30 μg) were precipitated using the ProteoExtract Kit (Merck, Darmstadt, Germany) according to the manufacturer's instructions. Precipitated proteins were solubilized in 25 mM ammonium bicarbonate containing 0.1% RapiGest (Waters, Eschborn, Germany) (80 °C, 15 min). Proteins were reduced by adding 5 mM DTT (45 min, 56 °C) and free cysteines alkylated with iodoacetamide (Sigma, Taufkirchen, Germany) (15 mM, 25 °C, 1 h in the dark). A 0.2 μg amount of porcine sequencing grade trypsin (Promega, Mannheim, Germany) was added, and the samples were incubated overnight at 37 °C. After digestion, RapiGest was hydrolyzed by adding 10 mM HCl (37 °C, 10 min), the resulting precipitate was removed by centrifugation (13000*g*, 15 min, 4 °C), and the supernatant was transferred into an autosampler vial for peptide analysis via LC-MS.

LC-MS Analysis of Tryptic Digests. Capillary liquid chromatography (LC) of tryptic peptides was performed with a Waters NanoAcquity UPLC system equipped with a 75 μm × 150 mm BEH C18 reversed phase column and a 2.6 μL PEEKSIL-sample loop (SGE, Darmstadt, Germany) as described.[56] The aqueous mobile phase (mobile phase A) was H_2O (LC-MS grade, Roth, Freiburg, Germany) with 0.1% formic acid. The organic mobile phase (mobile phase B) was 0.1% formic acid in acetonitrile (LC-MS grade, Roth). Samples (2.6 μL injection) were loaded onto the column in direct injection mode with 3% mobile phase B for 15 min at 400 nL/min, followed by an additional 10 min wash (3% B) for 10 min at 300 nL/min. Peptides were eluted from the column with a gradient from 3% to 35% mobile phase B over 90 min at 300 nL/min followed by a 20 min rinse of 80% mobile phase B. The column was immediately re-equilibrated at initial conditions (3% mobile phase B) for 20 min. [Glu^1]fibrinopeptide was used as lockmass at 300 fmol/μL. Lockmass solution was delivered from the auxiliary pump of the NanoAcquity system at 400 nL/min to the reference sprayer of the NanoLockSpray source. Samples were analyzed in three (NP-eluted proteins) or five (plasma proteins) technical replicates.

Mass spectrometry (MS) analysis of tryptic peptides was performed using a Waters Q-TOF Premier API system, operated in V-mode with typical resolving power of at least 10 000. All analyses were performed using positive mode ESI using a NanoLockSpray source. The lock mass channel was sampled every 30 s. The mass spectrometer was calibrated with a [Glu^1]fibrinopeptide solution (300 fmol/μL) delivered through the reference sprayer of the NanoLockSpray source. Accurate mass LC-MS data were collected in an alternating, low-energy (MS) and elevated energy (MS^E) mode of acquisition. The spectral acquisition time in each mode was 0.7 s with a 0.05 s interscan delay. In low-energy MS mode, data were collected at a constant collision energy of 3 eV. In MS^E mode, collision energy was ramped from 16 to 36 eV during each 0.7 s data collection cycle. One cycle of MS and MS^E data was acquired every 1.5 s. The radio frequency applied to the quadrupole mass analyzer was adjusted such that ions from *m/z* 300 to 1500 were efficiently transmitted, ensuring that any ions observed in the LC/MS^E data less than *m/z* 300 were known to arise from dissociations in the collision cell.

Bioinformatics, Database Searches, and Pathway Analysis. The continuum LC-MS^E data were processed and searched using the IDENTITY^E-Algorithm of ProteinLynx Global Server (PLGS) version 2.4. The resulting peptide and protein identifications were evaluated by the software using statistical models as described.[56] Protein identifications were assigned by searching the human taxon of the UniProtKB/SwissProt database (release 2010_09) supplemented with known possible contaminants and standard proteins (porcine trypsin, yeast enolase) using the precursor and fragmentation data afforded by the LC-MS acquisition method as described before.[56] The search parameter values for each precursor and associated fragment ions were set by the software using the measured mass error obtained from processing the raw continuum data. Peptide identifications were restricted to tryptic peptides with no more than one missed cleavage. Carbamidomethyl cysteine was set as fixed modification, and oxidized methionine, protein N-acetylation, and deamidation of asparagine and glutamine were searched as variable modifications. A database search was performed allowing a maximal mass deviation of 15 ppm for precursor ions and 30 ppm for fragment ions. For a valid protein identification, the following criteria had to be met: at least two peptides detected with a total of at least seven fragments. All reported peptide identifications provided by the IDENTITY^E-algorithm are correct with >95% probability.[57] The false positive rate for protein identification was set to 3% based on search of a 5× randomized database, which was generated automatically using PLGS 2.4 by randomizing the sequence of each entry. By using replication rate of identification as a filter, the false positive rate is further restricted to <0.2%. Alignment, normalization, and label-free quantification were performed using the Expression Module of PLGS2.4. Additional data processing including isoform/homology filtering and replicate filtering was performed by in-house developed software as described previously.[56] Pathway analysis was performed using GeneSpringGX11.0.2 (Waldbronn, Germany), IPA (Ingenuity System, Inc.; Redwood City, USA) as described.[54]

Statistical Analysis. For experiments' stating *p*-values, a paired Student's *t* test was performed as described.[58] *p*-values < 0.05 were considered as significant.

Immunoblotting. Immunoblotting was carried out according to standard procedures.[58] The following antibodies were used in the study: α-β-actin (1:2000, A2066; Sigma Aldrich, Taufkrichen, Germany), polyclonal α-gelsolin (1:200, SC-6405, Santa Cruz Biotechnology, Santa Cruz, CA, USA), monoclonal α-clusterin (1:200, SC-56079, Santa Cruz Biotechnology, Santa Cruz, CA, USA), monoclonal α-prothrombin (1:200, SC-73470, Santa Cruz Biotechnology, Santa Cruz, CA, USA), goat-anti-human IgG Ab conjugated with horseradish peroxidise (1:80.000, A0170, Sigma-Aldrich, Taufkirchen, Germany), goat-anti-rabbit IgG Ab conjugated with horseradish peroxidise (1:5000, Santa Cruz Biotechnology, Santa Cruz, CA, USA).

Supporting Information Available: Materials, experimental section, sample preparation, detailed description of LC-MS, as well as bioinformatic analysis. This material is available free of charge via the Internet at http://pubs.acs.org.

Acknowledgment. Grant support: DFG Priority Programm SPP1313/BIONEER/Silver-AG (R.S., L.T., R.Z., M.M.), DFG SFB490 (S.T., H.J.S.), BMBF NanoCare2-NanoKon (FKZ03X0100C), Mainz Screening Center/DFG INST371/5-1FUGG, Stiftung Rheinland-Pfalz für Innovation (FKZ899), ChemBioMed&Biomatics program, Forschungszentrum Immunologie University Mainz, Funds of the Chemical Industry, University Duisburg−Essen support program. We thank Sandra Friedl and Nathalie Philipp for excellent technical assistance.

REFERENCES AND NOTES

1. Riehemann, K.; Schneider, S. W.; Luger, T. A.; Godin, B.; Ferrari, M.; Fuchs, H. Nanomedicine--Challenge and Perspectives. *Angew. Chem., Int. Ed.* **2009**, *48*, 872–897.
2. McNeil, S. E. Nanoparticle Therapeutics A Personal Perspective. *Wiley Interdiscip. Rev. Nanomed. Nanobiotechnol.* **2009**, *1*, 264–271.
3. Murday, J. S.; Siegel, R. W.; Stein, J.; Wright, J. F. Translational Nanomedicine: Status Assessment and Opportunities. *Nanomedicine* **2009**, *5*, 251–273.
4. Ferrari, M. Nanogeometry: Beyond Drug Delivery. *Nat. Nanotechnol.* **2008**, *3*, 131–132.
5. Qian, X.; Peng, X. H.; Ansari, D. O.; Yin-Goen, Q.; Chen, G. Z.; Shin, D. M.; Yang, L.; Young, A. N.; Wang, M. D.; Nie, S. In Vivo Tumor Targeting and Spectroscopic Detection with Surface-Enhanced Raman Nanoparticle Tags. *Nat. Biotechnol.* **2008**, *26*, 83–90.
6. Alexiou, C.; Schmid, R. J.; Jurgons, R.; Kremer, M.; Wanner, G.; Bergemann, C.; Huenges, E.; Nawroth, T.; Arnold, W.; Parak, F. G. Targeting Cancer Cells: Magnetic Nanoparticles as Drug Carriers. *Eur. Biophys. J.* **2006**, *35*, 446–450.

7. Leszczynski, J. Bionanoscience: Nano Meets Bio at the Interface. *Nat. Nanotechnol.* **2010**, *5*, 633–634.
8. Adiseshaiah, P. P.; Hall, J. B.; McNeil, S. E. Nanomaterial Standards for Efficacy and Toxicity Assessment. *Wiley Interdiscip. Rev. Nanomed. Nanobiotechnol.* **2010**, *2*, 99–112.
9. Cedervall, T.; Lynch, I.; Lindman, S.; Berggard, T.; Thulin, E.; Nilsson, H.; Dawson, K. A.; Linse, S. Understanding the Nanoparticle-Protein Corona Using Methods to Quantify Exchange Rates and Affinities of Proteins for Nanoparticles. *Proc. Natl. Acad. Sci. U. S. A.* **2007**, *104*, 2050–2055.
10. Lynch, I.; Cedervall, T.; Lundqvist, M.; Cabaleiro-Lago, C.; Linse, S.; Dawson, K. A. The Nanoparticle-Protein Complex as a Biological Entity; a Complex Fluids and Surface Science Challenge for the 21st Century. *Adv. Colloid Interface Sci.* **2007**.
11. Walczyk, D.; Bombelli, F. B.; Monopoli, M. P.; Lynch, I.; Dawson, K. A. What the Cell "Sees" in Bionanoscience. *J. Am. Chem. Soc.* **2010**, *132*, 5761–5768.
12. Lundqvist, M.; Stigler, J.; Elia, G.; Lynch, I.; Cedervall, T.; Dawson, K. A. Nanoparticle Size and Surface Properties Determine the Protein Corona with Possible Implications for Biological Impacts. *Proc. Natl. Acad. Sci. U. S. A.* **2008**, *105*, 14265–14270.
13. Aggarwal, P.; Hall, J. B.; McLeland, C. B.; Dobrovolskaia, M. A.; McNeil, S. E. Nanoparticle Interaction with Plasma Proteins as It Relates to Particle Biodistribution, Biocompatibility and Therapeutic Efficacy. *Adv. Drug Delivery Rev.* **2009**, *61*, 428–437.
14. Verma, A.; Stellacci, F. Effect of Surface Properties on Nanoparticle-Cell Interactions. *Small* **2010**, *6*, 12–21.
15. Farrah, T.; Deutsch, E. W.; Omenn, G. S.; Campbell, D. S.; Sun, Z.; Bletz, J. A.; Mallick, P.; Katz, J. E.; Malmstrom, J.; Ossola, R.; *et al.* A High-Confidence Human Plasma Proteome Reference Set with Estimated Concentrations in Peptideatlas. *Mol Cell Proteomics* **2011**.
16. Jeong, S. K.; Kwon, M. S.; Lee, E. Y.; Lee, H. J.; Cho, S. Y.; Kim, H.; Yoo, J. S.; Omenn, G. S.; Aebersold, R.; Hanash, S.; *et al.* Biomarkerdigger: A Versatile Disease Proteome Database and Analysis Platform for the Identification of Plasma Cancer Biomarkers. *Proteomics* **2009**, *9*, 3729–3740.
17. Lacerda, S. H.; Park, J. J.; Meuse, C.; Pristinski, D.; Becker, M. L.; Karim, A.; Douglas, J. F. Interaction of Gold Nanoparticles with Common Human Blood Proteins. *ACS Nano* **2011**, *4*, 365–379.
18. Cedervall, T.; Lynch, I.; Foy, M.; Berggard, T.; Donnelly, S. C.; Cagney, G.; Linse, S.; Dawson, K. A. Detailed Identification of Plasma Proteins Adsorbed on Copolymer Nanoparticles. *Angew. Chem., Int. Ed.* **2007**, *46*, 5754–5756.
19. Hortin, G. L.; Sviridov, D.; Anderson, N. L. High-Abundance Polypeptides of the Human Plasma Proteome Comprising the Top 4 Logs of Polypeptide Abundance. *Clin Chem* **2008**, *54*, 1608–1616.
20. Omenn, G. S. Data Management and Data Integration in the Hupo Plasma Proteome Project. *Methods Mol. Biol.* **2011**, *696*, 247–257.
21. Nel, A. E.; Madler, L.; Velegol, D.; Xia, T.; Hoek, E. M.; Somasundaran, P.; Klaessig, F.; Castranova, V.; Thompson, M. Understanding Biophysicochemical Interactions at the Nano-Bio Interface. *Nat. Mater.* **2009**, *8*, 543–557.
22. Dobrovolskaia, M. A.; Clogston, J. D.; Neun, B. W.; Hall, J. B.; Patri, A. K.; McNeil, S. E. Method for Analysis of Nanoparticle Hemolytic Properties in Vitro. *Nano Lett* **2008**, *8*, 2180–2187.
23. Dobrovolskaia, M. A.; McNeil, S. E. Immunological Properties of Engineered Nanomaterials. *Nat. Nanotechnol.* **2007**, *2*, 469–478.
24. Xia, T.; Li, N.; Nel, A. E. Potential Health Impact of Nanoparticles. *Annu. Rev. Public Health* **2009**, *30*, 137–150.
25. Lynch, I.; Salvati, A.; Dawson, K. A. Protein-Nanoparticle Interactions: What Does the Cell See? *Nat. Nanotechnol.* **2009**, *4*, 546–547.
26. Dobrovolskaia, M. A.; Patri, A. K.; Zheng, J.; Clogston, J. D.; Ayub, N.; Aggarwal, P.; Neun, B. W.; Hall, J. B.; McNeil, S. E. Interaction of Colloidal Gold Nanoparticles with Human Blood: Effects on Particle Size and Analysis of Plasma Protein Binding Profiles. *Nanomedicine* **2009**, *5*, 106–117.
27. Dobrovolskaia, M. A.; Aggarwal, P.; Hall, J. B.; McNeil, S. E. Preclinical Studies to Understand Nanoparticle Interaction with the Immune System and Its Potential Effects on Nanoparticle Biodistribution. *Mol. Pharm.* **2008**, *5*, 487–495.
28. Mahmoudi, M.; Lynch, I.; Ejtehadi, M. R.; Monopoli, M. P.; Bombelli, F. B.; Laurent, S. Protein-Nanoparticle Interactions: Opportunities and Challenges. *Chem. Rev.* **2011**, DOI:10.1021/cr100440g.
29. Klein, J. Probing the Interactions of Proteins and Nanoparticles. *Proc. Natl. Acad. Sci. U. S. A.* **2007**, *104*, 2029–2030.
30. Monopoli, M. P.; Walczyk, D.; Campbell, A.; Elia, G.; Lynch, I.; Bombelli, F. B.; Dawson, K. A. Physical-Chemical Aspects of Protein Corona: Relevance to in Vitro and in Vivo Biological Impacts of Nanoparticles. *J. Am. Chem. Soc.* **2011**, *133*, 2525–2534.
31. Gessner, A.; Lieske, A.; Paulke, B. R.; Muller, R. H. Functional Groups on Polystyrene Model Nanoparticles: Influence on Protein Adsorption. *J. Biomed. Mater. Res. A* **2003**, *65*, 319–326.
32. Rocker, C.; Potzl, M.; Zhang, F.; Parak, W. J.; Nienhaus, G. U. A Quantitative Fluorescence Study of Protein Monolayer Formation on Colloidal Nanoparticles. *Nat. Nanotechnol.* **2009**, *4*, 577–580.
33. Deng, Z. J.; Mortimer, G.; Schiller, T.; Musumeci, A.; Martin, D.; Minchin, R. F. Differential Plasma Protein Binding to Metal Oxide Nanoparticles. *Nanotechnology* **2009**, *20*, 455101.
34. Min, Y. J.; Akbulut, M.; Kristiansen, K.; Golan, Y.; Israelachvili, J. The Role of Interparticle and External Forces in Nanoparticle Assembly. *Nat. Mater.* **2008**, *7*, 527–538.
35. Treuel, L.; Malissek, M.; Gebauer, J. S.; Zellner, R. The Influence of Surface Composition of Nanoparticles on Their Interactions with Serum Albumin. *Chemphyschem* **2010**, *11*, 3093–3099.
36. Gessner, A.; Lieske, A.; Paulke, B.; Muller, R. Influence of Surface Charge Density on Protein Adsorption on Polymeric Nanoparticles: Analysis by Two-Dimensional Electrophoresis. *Eur. J. Pharm. Biopharm.* **2002**, *54*, 165–170.
37. Dobrovolskaia, M. A.; Germolec, D. R.; Weaver, J. L. Evaluation of Nanoparticle Immunotoxicity. *Nat. Nanotechnol.* **2009**, *4*, 411–414.
38. Radomski, A.; Jurasz, P.; Alonso-Escolano, D.; Drews, M.; Morandi, M.; Malinski, T.; Radomski, M. W. Nanoparticle-Induced Platelet Aggregation and Vascular Thrombosis. *Br. J. Pharmacol.* **2005**, *146*, 882–893.
39. Vaisar, T.; Pennathur, S.; Green, P. S.; Gharib, S. A.; Hoofnagle, A. N.; Cheung, M. C.; Byun, J.; Vuletic, S.; Kassim, S.; Singh, P.; et al. Shotgun Proteomics Implicates Protease Inhibition and Complement Activation in the Antiinflammatory Properties of Hdl. *J. Clin. Invest.* **2007**, *117*, 746–756.
40. Reilly, M. P.; Tall, A. R. Hdl Proteomics: Pot of Gold or Pandora's Box? *J. Clin. Invest.* **2007**, *117*, 595–598.
41. Hellstrand, E.; Lynch, I.; Andersson, A.; Drakenberg, T.; Dahlback, B.; Dawson, K. A.; Linse, S.; Cedervall, T. Complete High-Density Lipoproteins in Nanoparticle Corona. *FEBS J.* **2009**, *276*, 3372–3381.
42. Zensi, A.; Begley, D.; Pontikis, C.; Legros, C.; Mihoreanu, L.; Buchel, C.; Kreuter, J. Human Serum Albumin Nanoparticles Modified with Apolipoprotein a-I Cross the Blood-Brain Barrier and Enter the Rodent Brain. *J. Drug Targeting* **2010**, *18*, 842–848.
43. Benderly, M.; Boyko, V.; Goldbourt, U. Apolipoproteins and Long-Term Prognosis in Coronary Heart Disease Patients. *Am. Heart J.* **2009**, *157*, 103–110.
44. Thambisetty, M.; Simmons, A.; Velayudhan, L.; Hye, A.; Campbell, J.; Zhang, Y.; Wahlund, L. O.; Westman, E.; Kinsey, A.; Guntert, A.; *et al.* Association of Plasma Clusterin Concentration with Severity, Pathology, and Progression in Alzheimer Disease. *Arch. Gen. Psychiatry* **2010**, *67*, 739–748.

45. Bucki, R.; Levental, I.; Kulakowska, A.; Janmey, P. A. Plasma Gelsolin: Function, Prognostic Value, and Potential Therapeutic Use. *Curr. Protein Pept. Sci.* **2008**, *9*, 541–551.
46. DiNubile, M. J. Plasma Gelsolin as a Biomarker of Inflammation. *Arthritis Res. Ther.* **2008**, *10*, 124.
47. Spinardi, L.; Witke, W. Gelsolin and Diseases. *Subcell Biochem.* **2007**, *45*, 55–69.
48. Casals, E.; Pfaller, T.; Duschl, A.; Oostingh, G. J.; Puntes, V. Time Evolution of the Nanoparticle Protein Corona. *ACS Nano* **2010**, *4*, 3623–3632.
49. Dell'Orco, D.; Lundqvist, M.; Oslakovic, C.; Cedervall, T.; Linse, S. Modeling the Time Evolution of the Nanoparticle-Protein Corona in a Body Fluid. *PLoS One* **2010**, *5*, e10949.
50. Jiang, X.; Weise, S.; Hafner, M.; Rocker, C.; Zhang, F.; Parak, W. J.; Nienhaus, G. U. Quantitative Analysis of the Protein Corona on Fept Nanoparticles Formed by Transferrin Binding. *J. R. Soc. Interface* **2010**, *7*), S5–S13.
51. Moreau, J. W.; Weber, P. K.; Martin, M. C.; Gilbert, B.; Hutcheon, I. D.; Banfield, J. F. Extracellular Proteins Limit the Dispersal of Biogenic Nanoparticles. *Science* **2007**, *316*, 1600–1603.
52. Kasper, J.; Hermanns, I.; Bantz, C.; Maskos, M.; Stauber, R. H.; Pohl, C.; Unger, R.; Kirkpatrick, J. C. Inflammatory and Cytotoxic Responses of an Alveolar-Capillary Coculture Model to Silica Nanoparticles: Comparison with Conventional Monocultures. *Particle Fiber Toxicol.* **2011**, *8*, 1–16.
53. Scherer, C.; Noskov, S.; Utech, S.; Bantz, C.; Mueller, W.; Krohne, K.; Maskos, M. Characterization of Polymer Nanoparticles by Asymmetrical Flow Field Flow Fractionation (Af-Fff). *J. Nanosci. Nanotechnol.* **2010**, *10*, 6834–6839.
54. Bier, C.; Knauer, S. K.; Klapthor, A.; Schweitzer, A.; Rekik, A.; Kramer, O. H.; Marschalek, R.; Stauber, R. H. Cell-Based Analysis of Structure-Function Activity of Threonine Aspartase 1. *J. Biol. Chem.* **2011**, *286*, 3007–3017.
55. Thiel, U. J.; Feltens, R.; Adryan, B.; Gieringer, R.; Brochhausen, C.; Schuon, R.; Fillies, T.; Grus, F.; Mann, W. J.; Brieger, J. Analysis of Differentially Expressed Proteins in Oral Squamous Cell Carcinoma by Maldi-Tof Ms. *J. Oral Pathol. Med.* **2010**, *40*, 369–379.
56. Tenzer, S.; Wee, E.; Burgevin, A.; Stewart-Jones, G.; Friis, L.; Lamberth, K.; Chang, C. H.; Harndahl, M.; Weimershaus, M.; Gerstoft, J.; *et al.* Antigen Processing Influences Hiv-Specific Cytotoxic T Lymphocyte Immunodominance. *Nat. Immunol.* **2009**, *10*, 636–646.
57. Silva, J. C.; Gorenstein, M. V.; Li, G. Z.; Vissers, J. P.; Geromanos, S. J. Absolute Quantification of Proteins by Lcmse: A Virtue of Parallel Ms Acquisition. *Mol. Cell Proteomics* **2006**, *5*, 144–156.
58. Knauer, S. K.; Heinrich, U. R.; Bier, C.; Habtemichael, N.; Docter, D.; Helling, K.; Mann, W. J.; Stauber, R. H. An Otoprotective Role for the Apoptosis Inhibitor Protein Survivin. *Cell Death Dis.* **2010**, *1*, e51.